

## REFERENCES AND NOTES

- W. F. Post *et al.*, *Am. Sci.* **78**, 310 (1990); J. I. Hedges, *Mar. Chem.*, in press.
- L. R. Pomeroy, *Bioscience* **24**, 499 (1974); F. Azam *et al.*, *Mar. Ecol. Progr. Ser.* **10**, 257 (1983).
- E. Goldberg and A. Bard, *Appl. Geochem.* **3**, 3 (1988).
- P. J. Williams, in *Chemical Oceanography*, J. P. Riley and G. Skirrow, Eds. (Academic Press, London, 1975), pp. 301–363.
- P. M. Williams and E. R. M. Druffel, *Oceanography* **1**, 14 (1988).
- E. M. Thurman, *Organic Geochemistry of Natural Waters* (Nijhoff/Junk, Dordrecht, the Netherlands, 1985), chap. 10.
- M. Cheryan, *Ultrafiltration Handbook* (Technomic, Lancaster, 1986), chap. 1.
- S. Chiswell, E. Firing, D. Karl, R. Lukas, C. Winn, *School of Ocean and Earth Science and Technology Technical Report 1* (University of Hawaii, Honolulu, 1990).
- Y. Sugimura and Y. Suzuki, *Mar. Chem.* **24**, 105 (1988).
- Analyses of DOC were made using a Pt catalyst (0.5% Pt on Al<sub>2</sub>O<sub>3</sub> support) at 680°C. Samples were filtered (0.2- $\mu$ m pore size), acidified (10% H<sub>3</sub>PO<sub>4</sub>) to a pH of ~2, and purged for 5 min immediately before analysis with the same ultrahigh purity oxygen that was used to operate the TOC analyzer. The water blank ( $4 \pm 2 \mu\text{M C}$ ) and instrument blank ( $22 \pm 3 \mu\text{M C}$ ) were measured at the time of sample analysis [R. Benner and M. Strom, *Mar. Chem.*, in press].
- D. J. Carlson, M. L. Brann, T. H. Mague, L. M. Mayer, *Mar. Chem.* **16**, 155 (1985).
- K. J. Meyers-Schulte and J. I. Hedges, *Nature* **321**, 61 (1986).
- T. W. Walsh, *Mar. Chem.* **26**, 295 (1989).
- J. I. Hedges, B. A. Bergamaschi, R. Benner, *ibid.*, in press.
- Y. Suzuki, Y. Sugimura, T. Itoh, *ibid.* **16**, 83 (1985).
- Solid-state NMR spectra were obtained using a Chemagnetics Inc. M-100 spectrometer. Conditions were chosen to insure that the NMR signal intensities quantitatively represented the carbon types observed in the samples [M. A. Wilson, *NMR Techniques and Applications in Geochemistry and Soil Chemistry* (Pergamon, Oxford, 1987)]. Approximately 50,000 transients, having pulse delays of 1 s, sweep widths of 14 kHz, contact times of 1 ms, and 90° <sup>1</sup>H pulses of 5.8 s were acquired at a field strength of 2.35 Tesla.
- P. M. Williams and E. R. M. Druffel, *Nature* **330**, 246 (1987).
- D. H. Stuermer and J. R. Payne, *Geochim. Cosmochim. Acta* **40**, 1109 (1976); R. B. Gagosian and D. H. Stuermer, *Mar. Chem.* **5**, 605 (1977); G. R. Harvey, D. A. Boran, L. A. Chesal, J. M. Tokar, *ibid.* **12**, 119 (1983); M. A. Wilson, A. H. Gillam, P. J. Collin, *Chem. Geol.* **40**, 187 (1983); R. Malcolm, *Anal. Chim. Acta* **232**, 19 (1990).
- J. I. Hedges, P. G. Hatcher, J. R. Ertel, K. J. Meyers-Schulte, *Geochim. Cosmochim. Acta*, in press.
- C. M. Burney and J. McN. Sieburth, *Mar. Chem.* **5**, 15 (1977).
- J. D. Pakulski and R. Benner, in preparation.
- C. M. Burney, K. M. Johnson, D. M. Lavoie, J. McN. Sieburth, *Deep-Sea Res.* **26A**, 1267 (1979).
- C. M. Burney, P. G. Davis, K. M. Johnson, J. McN. Sieburth, *Mar. Biol.* **67**, 311 (1982).
- We thank the scientists, captain, and crew on the R.V. *Alpha Helix* for assistance collecting water samples and D. Karl and R. Lukas for providing logistical support. We are grateful to M. Strom for assistance with DOC measurements and ultrafiltration experiments. We also acknowledge J. Schroyer for help with integration of the NMR spectra. This research was supported by grants from the National Science Foundation (BSR 8910766 and OCE 9102407 to R.B. and BSR 8718423 and OCE 9102150 to J.H.). Contribution 830 of the University of Texas Marine Science Institute and contribution 1918 of the University of Washington School of Oceanography.

12 November 1991; accepted 31 January 1992

## Percolation Theory, Thermoelasticity, and Discrete Hydrothermal Venting in the Earth's Crust

L. N. GERMANOVICH\* AND ROBERT P. LOWELL†

As hydrothermal fluid ascends through a network of cracks into cooler crust, heat is transferred from the fluid to the adjacent rock. The thermal stresses caused by this heating close cracks that are more or less vertical. This heating may affect network connections and destroy the permeable crack network. Thermoelastic stresses caused by a temperature difference of ~100°C can decrease the interconnectivity of a crack network to the percolation threshold. If the temperature is slightly less, thermoelastic stresses may focus the discharge in hydrothermal systems into discrete vents.

FLUID CIRCULATION IN HYDROTHERMAL systems is controlled by the distribution of rock permeability in space and time. In igneous and metamorphic rocks the permeability is controlled by fractures (1), and discharge in both continental and submarine hydrothermal systems appears to be localized by fault zones (2). On land, the fault-controlled discharge may emerge as discrete warm or hot springs; at mid-ocean ridge crests, high-temperature discharge occurs through orifices  $\approx 10$  cm in diameter as sulfide-laden black smoker plumes with a temperature  $\approx 350^\circ\text{C}$  (3).

It is not clear how hydrothermal upflow in a fault zone is focused into discrete vents or what factors control the spacing of vents

along the fault zone. Deposits of silica and other minerals are common in hydrothermal systems, and it is generally believed that such deposits clog fractures and decrease permeability at shallow levels in hydrothermal systems (4). However, quantitative analysis of this process is extremely difficult. Models of porosity reduction due to chemical deposition suggest that the process is inefficient (5). It may be that chemical deposition alone may not cause flow to be focused into discrete vents.

In this report, we examine the role of thermoelastic stresses in a hydrothermal upflow zone as a mechanism for focusing. The conceptual picture (Fig. 1) is that, as hydrothermal fluid heated at depth ascends into the cooler, shallow crust, heat is transferred from the fluid in the cracks to the adjacent rock. Because the heated zone is always surrounded by cooler areas, this heating imposes horizontal thermal stresses on the rock that can close cracks. If enough crack connections are destroyed so that the crack

network falls to near the percolation threshold, then only a few pathways would be open to the surface and the flow would be directed through them. We derive an expression for the closure of cracks by thermoelastic stresses and then estimate how much heating is required to decrease the interconnectivity of the crack network to the percolation threshold. Thermoelastic stresses may act in concert with chemical deposition to focus the flow into discrete vents.

Earlier work (6) showed that, if hot fluid flowed in a single, planar fracture 1 mm wide, the fracture could close within 0.5 year because of thermal expansion of the adjacent rock. Lowell (7) extended this result to a set of parallel planar fractures of uniform width and spacing. However, critical questions remain concerning thermoelastic effects in rocks containing a random crack network.

The sizes, orientations, number density, aspect ratios, and other properties of cracks in hydrothermal systems are uncertain. We therefore use an order of magnitude analysis to examine the role of thermoelastic effects in discharge zones and make a number of simplifying assumptions that are consistent with this approach. We assume that (i) for calculating the influence of thermoelastic stresses, each crack can be treated as separate but located in a rock volume with some effective elastic properties; (ii) the three-dimensional (3-D) cracks have the shape of a thin spheroid described in terms of an aspect ratio  $x = a/b$ , where  $a$  is the small semi-axis and  $b$  is the large one; (iii) the thermoelastic stress field on the cracks has two equal

School of Earth and Atmospheric Sciences, Georgia Institute of Technology, Atlanta, GA 30332.

\*Present address: School of Petroleum and Geological Engineering, University of Oklahoma, Norman, OK 73019.

†To whom correspondence should be addressed.

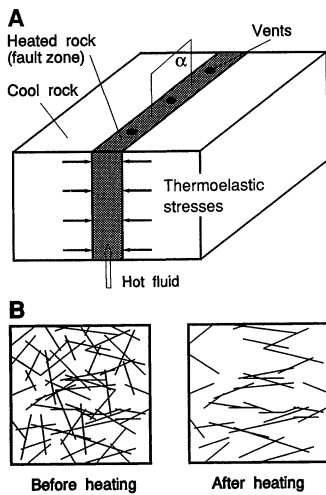


**Fig. 1.** (A) Schematic of hydrothermal upflow in a fault zone showing thermoelastic stresses. (B) Cross-sectional view of part of the fault zone ( $\alpha$ ) depicting the distribution of open cracks before and after heating.

horizontal components,  $\sigma$  (8); (iv) flow essentially takes place along a subnetwork of the less resistant, widest cracks (9), so we can consider this subnetwork to be the main network from the beginning; (v) roughness of the crack walls can be neglected, because, even if the fracture remains partially open because of asperities, the permeability of the fracture would be several orders of magnitude less than that of the open fracture, provided the roughness is on a scale that is at least an order of magnitude less than the original crack aperture (10); and (vi) the cracks are randomly oriented in space; the aspect ratio  $x$  is independent of orientation and ranges between 0 and some small finite value  $\epsilon$ .

Assumption (vi) can be expressed by normalized distribution functions  $f(x)$  and  $\phi(\beta)$  for aspect ratio  $x$  and orientation angle  $\beta$ , respectively:

$$f(x) = \begin{cases} 0 & \text{if } x \notin [0, \epsilon] \\ N_0/\epsilon & \text{if } x \in [0, \epsilon] \end{cases} \quad (1)$$

$$\phi(\beta) = \begin{cases} 0 & \text{if } \beta \notin [-\pi/2, \pi/2] \\ 1/\pi & \text{if } \beta \in [-\pi/2, \pi/2] \end{cases} \quad (2)$$

where  $N_0$  is the initial crack concentration.

Assumptions (i) and (ii) permit us to use the simple formula  $\sigma = \alpha ET/(1 - \nu)$  for the thermoelastic stress, where  $E$  is Young's modulus,  $T$  is the temperature difference between the fluid and cool rock,  $\alpha$  is the linear coefficient of thermal expansion, and  $\nu$  is Poisson's ratio (11). For a single crack oriented at an angle  $\beta$  to the horizontal plane, only the component of stress normal to the crack plane is effective at closing the crack. This stress,  $\sigma_n$ , can be written  $\sigma_n = \sigma \sin^2 \beta$ .

A penny-shaped spheroidal crack of as-

pect ratio  $x$  will be closed by the stress  $\sigma_n$  if  $x \leq (4/\pi)(1 - \nu^2)\sigma_n/E$  (12). Thus, for a given stress, all cracks with  $x \leq x_c$  are closed where

$$x_c = T_* \sin^2 \beta \quad (3)$$

and  $T_* = (4/\pi)(1 + \nu)\alpha T$  is a dimensionless temperature. Because  $0 \leq x \leq \epsilon$ , Eq. 3 shows that, as  $T_*$  becomes greater than  $\epsilon$ ,  $\sin^2 \beta$  must be less than unity. Thus heating will preferentially close cracks that are more or less vertical.

The number density of open cracks after heating,  $N(T_*)$ , divided by the initial value  $N_0$  is found by integrating the distribution functions given by Eqs. 1 and 2 over the region of open cracks. The result is

$$N(T_*)/N_0 = \begin{cases} 1 - T_*/2\epsilon & \text{if } T_* \leq \epsilon \\ (2/\pi)[(1 - T_*/2\epsilon)\sin^{-1}\sqrt{\epsilon/T_*} \\ + (1/2)\sqrt{T_*/\epsilon - 1}] & \text{if } T_* \geq \epsilon \end{cases} \quad (4)$$

Then the average distance between cracks  $L$  compared to the average distance  $L_0$  before heating is  $L(T_*)/L_0 \approx [N_0/N(T_*)]^{1/3}$ .

Equation 4 shows that the number density of open cracks decreases as the temperature of the rock increases. This corresponds to an increase in the average distance between open cracks.  $L/L_0$  is proportional to  $(T_*/\epsilon)^{1/6}$  as the temperature becomes high, indicating that the focusing of the flow by simply heating the rock is weakly dependent on temperature. Moreover, all cracks were considered in the analysis that led to Eq. 4, whereas only a few of the cracks contribute to the permeability of the crack network, because most of the cracks form finite isolated clusters and dead ends. We therefore apply percolation theory [for example, (13, 14)] to address the possibility that thermoelastic stresses due to heating, which preferentially closes cracks that are more or less vertical, may affect network connections and thereby destroy the permeable crack network.

Consider a random distribution of sites (cracks) of different sizes and orientations. The classical percolation problem is concerned with the first appearance of an infinite connected cluster (the percolation threshold) as the number of random sites increases. In our situation, however, we initially consider a distribution of cracks that is above the percolation threshold. During heating, some cracks are closed and the spatial orientation of the remaining open cracks might be restricted to the interval  $-\beta_c \leq \beta \leq \beta_c$ , as determined by Eq. 3 (15). We wish to determine when the crack distribution falls below the percolation threshold.

We follow a common view [for example, (13, 14)] and suppose that near the percola-

tion threshold for the random site problem the characteristic cell size (or nodal spacing) of the backbone network,  $R$ , that is thought to occur within the infinite cluster can be written:

$$R \propto |B - B_c|^{-\gamma} \quad (5)$$

where  $B$  is the mean number of bonds per site for a given percolation object,  $B_c$  is the critical mean number of bonds per site at the percolation threshold, and  $\gamma$  is an invariant that depends only on the dimensionality of the problem. For 3-D problems  $\gamma \approx 0.9$ , whereas for 2-D problems  $\gamma \approx 1.3$ . Two sites (percolation object centers) are considered to be bonded if the corresponding objects intersect each other, which means that  $B$  is the average number of intersections per percolation object.

To determine the percolation threshold for a crack system subjected to thermoelastic stresses, we must determine  $B$  and  $B_c$  for the crack network, substitute the results into Eq. 5, and determine when  $R$  approaches infinity. As heating reduces the number of open, connected cracks, the percolation threshold is approached from above. At the threshold, there is one continuous pathway; below the percolation threshold, there is no permeability. We can thus interpret the approach to the percolation threshold from above as corresponding to the focusing of the hydrothermal discharge into discrete vents.

Balberg *et al.* (16) suggested that  $B$  can be expressed as

$$B = N \langle V_c \rangle \quad (6)$$

where  $N$  is the number of sites per unit volume, and  $\langle V_c \rangle$  is the average excluded volume, that is, the volume around one percolation object within which a second object must have its center in order for the two sets to intersect (17). The average is taken over the sizes and orientations of all objects. A number of numerical simulations has shown that Eq. 6 is likely to hold for any object shape (18). Generally,  $B$  is a quasi-invariant that depends on the shape of the objects but not on the distribution of their size or orientation (19).

We first obtain an expression for  $\langle V_c \rangle$ . We assume that circular disks are a good enough approximation for cracks, because small aperture is not important at the percolation threshold. For a pair of circular disks whose plane makes an angle  $\theta$  and whose radii are  $r_1$  and  $r_2$ , the excluded volume is  $V_c = 2\pi r_1 r_2 (r_1 + r_2) \sin \theta$  (17). After averaging over all the crack radii and orientations, we have

$$\langle V_c \rangle = 4\pi \langle r^2 \rangle \langle r \rangle \langle \sin \theta \rangle \quad (7)$$

where  $\langle \rangle$  represents the mean. From Eq. 3, the orientation angle for open cracks is

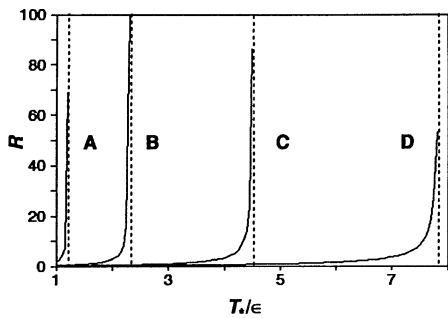


**Fig. 2.** Characteristic size of network cell  $R$  for an anisotropic crack distribution as a function of the parameter  $T_*/\epsilon$  for  $B_c = 2$  (from Eqs. 4 and 10). Curves A, B, C, and D correspond to values of  $\Omega_0$  of 0.5, 1.0, 2.0, and 3.5, respectively.

$$-\beta_c \leq \beta \leq \beta_c = \begin{cases} \pi/2 & \text{if } T_* \leq \epsilon \\ \sin^{-1} \sqrt{\epsilon/T_*} & \text{if } T_* > \epsilon \end{cases} \quad (8)$$

Using the general approximation given by Balberg (16) for  $\langle \sin\theta \rangle$  that we apply for the range of angle given by Eq. 8, we obtain  $\langle V_c \rangle$  for an anisotropic crack distribution:

$$\langle V_c \rangle \approx [5\pi \langle r^2 \rangle \langle r \rangle / (2\beta_c^2)] [2\beta_c - \sin(2\beta_c)] \quad (9)$$

$N\langle V_c \rangle$  is the average number of intersections per crack at the percolation threshold (20), and this number must exceed a critical value. We take the value  $B_c \approx 2$ , given by numerical studies (21, 22). Substituting Eqs. 6 and 9 in Eq. 5, we now have

$$R \propto \frac{[N(T_*)/N_0] \Omega_0 [5\pi / (2\beta_c^2)] [2\beta_c - \sin(2\beta_c)] - 2}{\gamma} \quad (10)$$

where  $\Omega_0 = N_0 \langle r^3 \rangle$  is the initial dimensionless crack concentration (23),  $N(T_*)/N_0$  is given by Eq. 4, and we have approximated  $\langle r^2 \rangle \langle r \rangle \approx \langle r^3 \rangle$ . As shown in Fig. 2, there is a critical dimensionless temperature  $T_*/\epsilon$  with a value of  $\approx 2.25$  for  $\Omega_0 = 1.0$ .

It is clear that  $\Omega_0 > \Omega_c$ , where  $\Omega_c$  is the critical crack concentration before heating when cracks are randomly oriented. In this case the excluded volume  $\langle V_c \rangle = \pi^2 \langle r^2 \rangle \langle r \rangle$  (24). Because  $B_c \approx 2$ ,  $\Omega_c \approx 0.2$ , which is the lower boundary for  $\Omega_0$ . For  $\Omega_0 = 1.0$ , the average crack length is twice the average crack spacing. This value corresponds to a high degree of rock disconnection and can be taken as an upper bound  $\Omega_u$  for  $\Omega_0$ . So  $\Omega_c < \Omega \leq \Omega_u$  and substituting  $T_*$  from Eq. 3 gives an order of magnitude relation for the threshold temperature  $0 < T_c \leq \epsilon/\alpha$  for the breakdown of percolation. Even if the typical crack length were three times the typical distance between crack centers ( $\Omega_0 \approx 3.5$ ), the result would be the same to an order of magnitude (Fig. 2).

For a characteristic  $\alpha$  for rocks of  $10^{-5} \text{ } ^\circ\text{C}^{-1}$ ,  $T_c$  is less than  $1000^\circ\text{C}$  for  $\epsilon < 10^{-2}$ . Such values for  $\epsilon$  are consistent with typical crack aspect ratios at least at the

laboratory scale (25) and appear reasonable for the macroscopic scale. For example, if fluid  $100^\circ\text{C}$  hotter than the rock enters a set of uniformly distributed cracks that have aspect ratios up to  $\epsilon = 10^{-3}$  and randomly distributed orientation angles, the crack system with  $\Omega_0 \leq 1.0$  will be self-sealed as a result of the thermal stress.

The above result indicates that thermoelastic stresses can exert significant control on the flow of hot fluids through cooler, cracked rocks, but there are few direct data to support this result. A study on the East Pacific Rise (26, 27) showed that high-temperature hydrothermal activity was confined to fissures within a zone  $\approx 60$  m wide at the axial graben. Active sites were spaced approximately 200 to 300 m apart along a 20-km length of ridge crest. Individual active areas were 10 to 30 m long and 5 to 10 m wide (27). It is conceivable that, when a pulse of activity began, a temperature contrast of  $\sim 100^\circ\text{C}$  may have developed between the hot ascending fluid and the surrounding rocks that led to further focusing of the flow and to the spacing of the active sites along the fault zone.

In the Basin and Range of the western United States, hydrothermal activity appears to be controlled by deep faults (28). Hose and Taylor (28) pointed out a number of warm springs in the Double Hot Springs-Black Rock area, separated by about 1.5 km, that discharge along a 10-km linear trend. Numerous deposits of silica and travertine suggest the likely importance of chemical sealing of permeability, but thermoelastic stresses may have also contributed to focusing the flow into discrete outlets. The focusing effect is greater, the closer the initial crack concentration is the critical value  $\Omega_c$ .

It is generally believed that chemical deposition is a major cause of permeability loss in hydrothermal systems (4). In future studies, it will be useful to simultaneously incorporate chemical and thermoelastic processes into hydrothermal models. If a law for the closure of a single crack by chemical deposition were available, the formalism used in this report could be applied to this problem as well. During chemical sealing, however, the crack distribution will remain isotropic, if it was so originally.

Thermoelastic processes may also lead to episodic venting. Suppose a loss of percolation does occur in a part of a hydrothermal system as a result of thermoelastic sealing. As the sealed part cools, the fractures will reopen and another pulse of hot fluid can flow through. If cooling is by conduction through the walls of the fault, the pulsation time is given roughly by the characteristic cooling time  $\tau \approx h^2/a$ , where  $h$  is the thick-

ness and  $a$  is the thermal diffusivity in the fault zone, respectively. For geologically reasonable values of  $h \approx 10$  m and  $a = 10^{-6} \text{ m}^2/\text{s}$ ,  $\tau \approx 10$  years.

Our discussion has focused on fault zones, that is, systems with finite widths, whereas the result derived above is for an infinite 3-D space. We do not know of any calculations applicable to this problem but suspect that the values for the main parameters of percolation theory,  $B_c$  and  $\gamma$ , lie somewhere between those for pure 2-D and 3-D problems, because, in comparison to 2-D problems, we have an additional degree of freedom, but, in comparison to the 3-D problem, the freedom is not full.

For the 2-D crack problem,  $B_c \approx 3$  to 4 (21). A higher value of  $B_c$  will lower the estimate of the critical temperature somewhat. We prefer the 3-D value  $B_c \approx 2$ , because, even if the characteristic cell size of the main percolation network is larger than the width of the fault zone, that width is much bigger than the typical crack size. Hence, from the local point of view the crack network is 3-D.

In contrast,  $\gamma$  reflects the global properties of the space and does not depend on the local structure of the network (13). The closer the crack concentration is to the percolation threshold, the larger the characteristic size of the network cell. For the problem described here, the characteristic size eventually becomes much greater than the fault zone width, so the situation becomes effectively 2-D, from the global point of view. For this reason we prefer  $\gamma = 1.3$ , corresponding to the 2-D case. In any event, it is only important in the present consideration that Eq. 5 remains applicable as  $\gamma$  changes from 0.9 to 1.3 while the characteristic size of the network cell changes from much less to much more than the fault zone width. These uncertainties do not affect the order of magnitude of the result derived here.

#### REFERENCES AND NOTES

1. W. F. Brace, *Int. J. Rock Mech. Min. Sci.* **17**, 241 (1980); *J. Geophys. Res.* **89**, 4327 (1984).
2. W. A. Hobba, Jr., D. W. Fisher, F. J. Pearson, Jr., J. C. Chemerys, *U.S. Geol. Surv. Prof. Pap.* 1044-E (1979); P. A. Rona and J. Karson, *Geol. Soc. Am. Bull.* **102**, 1635 (1990).
3. F. N. Spiess *et al.*, *Science* **207**, 1421 (1980).
4. D. E. White, M. W. Brannock, K. J. Murata, *Geochim. Cosmochim. Acta* **10**, 27 (1956); R. O. Fournier, in *Reviews in Economic Geology*, B. R. Berger and P. M. Bethke, Eds. (Economic Geology, El Paso, TX, 1985), vol. 2, pp. 45-62.
5. J. Walder and A. Nur, *J. Geophys. Res.* **89**, 11539 (1984).
6. G. Bodvarsson, in *Proceedings of 2nd United Nations Symposium on the Development and Use of Geothermal Resources*, San Francisco, 20 to 29 May 1975 (Government Printing Office, Washington, DC, 1975), pp. 903-907.
7. R. P. Lowell, *Geophys. Res. Lett.* **17**, 709 (1990).

8. For a fault zone in the earth's crust, the two horizontal stresses may be unequal, but the assumption of equality does not change the order of magnitude of the results.
9. E. Charlaix, E. Guyon, E. Roux, *Transp. Porous Media* **2**, 31 (1987).
10. L. J. Pyrak-Nolte, N. G. W. Cook, D. D. Nolte, *Geophys. Res. Lett.* **5**, 1247 (1988).
11. This well-known formula is sufficient, provided the faulted rocks are much more deformable than the adjacent rocks, which is the case here because the faulted rocks presumably contain more cracks. The applicability of this formula to rock heating is discussed in L. N. Germanovich, A. P. Dmitriev, S. A. Goncharov, *Thermomechanics of Rock Fracture* (Gordon and Breach, London, in press).
12. I. N. Sneddon and M. Lowengrub, *Crack Problems in the Classical Theory of Elasticity* (Wiley, New York, 1969).
13. B. I. Shklovskii and A. L. Efros, *Electronic Properties of Doped Semiconductors* (Springer-Verlag, New York, 1984), chap. 5.
14. D. Stauffer, *Introduction to Percolation Theory* (Taylor and Francis, London, 1985).
15. As a result, we cannot apply a model of stress-induced anisotropy that is based on two sets of perpendicular cracks as in C. M. Sayers [*Transp. Porous Media* **5**, 287 (1990)].
16. I. Balberg, C. H. Anderson, S. Alexander, N. Wagner, *Phys. Rev. B* **30**, 3933 (1984).
17. L. Onsager, *Ann. N.Y. Acad. Sci.* **51**, 627 (1949).
18. I. Balberg, *Phys. Rev. B* **31**, 4053 (1985), and references therein.
19. ———, *Philos. Mag.* **B 56**, 991 (1987).
20.  $N(V_c)$  means the average number of disk centers in the volume  $(V_c)$ , but, if two disk centers are inside  $(V_c)$ , it is not necessary that the disks will intersect each other. That  $NV_c$  is also equal to the average number of intersections per crack can be strictly proved for the case of 3-D percolation in disk-like cracks and for any other percolation object shape that can be described by a finite number of parameters. It is likely that the statement is true in any case.
21. P. C. Robinson, *J. Phys. A* **17**, 2823 (1984).
22. E. Charlaix, *ibid.* **19**, L533 (1986).
23. R. L. Salganik, *Mech. Solids* **8**, 135 (1973).
24. E. Charlaix, E. Guyon, N. Rivier, *Solid State Commun.* **50**, 999 (1984). This is a particular case of Eq. 7 because  $(\sin\theta) = \pi/4$  for  $\beta_c = \pi/2$  (16).
25. K. Hadley, *J. Geophys. Res.* **81**, 3483 (1976).
26. P. Gente, J. M. Auzende, V. Renard, Y. Fouquet, D. Bideau, *Earth Planet. Sci. Lett.* **78**, 224 (1986).
27. Y. Fouquet, G. Auclair, P. Cambon, J. Etoubleau, *Mar. Geol.* **84**, 145 (1988).
28. R. K. Hose and B. E. Taylor *U.S. Geol. Surv. Open File Rep.* 74-271 (1974).
29. We appreciate the many helpful comments by the reviewers of earlier versions of this manuscript. This work was supported by the National Science Foundation under grant OCE 9012665 to R.P.L. L.N.G. thanks Parsons Brinckerhoff-KBB, Inc., Houston, TX, for supporting this work while he was in their employ.

8 October 1991; accepted 15 January 1992

## Voltage-Dependent Calcium Channels in Plant Vacuoles

OMAR PANTOJA, ANGIE GELLI, EDUARDO BLUMWALD\*

Free calcium ( $\text{Ca}^{2+}$ ) in the cytoplasm of plant cells is important for the regulation of many cellular processes and the transduction of stimuli. Control of cytoplasmic  $\text{Ca}^{2+}$  involves the activity of pumps, carriers, and possibly ion channels. The patch-clamp technique was used to study  $\text{Ca}^{2+}$  channels in the vacuole of sugar beet cells. Vacuolar currents showed inward rectification at negative potentials, with a single-channel conductance of 40 picosiemens and an open probability dependent on potential. Channels were inhibited by verapamil and lanthanum. These channels could participate in the regulation of cytoplasmic  $\text{Ca}^{2+}$  by sequestering  $\text{Ca}^{2+}$  inside the vacuole.

FLUCTUATIONS IN THE AMOUNT OF cytoplasmic calcium ( $\text{Ca}^{2+}_{\text{cyt}}$ ) are involved in the regulation of many cellular processes in animal cells (1); thus the concentrations of  $\text{Ca}^{2+}_{\text{cyt}}$  must be under tight control. In most animal cells, increases in the amount of  $\text{Ca}^{2+}_{\text{cyt}}$  occur as  $\text{Ca}^{2+}$  moves through selective channels in the plasma membrane and in the membrane of intracellular organelles (mainly the endoplasmic reticulum) (1). Decreases in the amount of  $\text{Ca}^{2+}_{\text{cyt}}$  occur primarily through the activity of  $\text{Ca}^{2+}$  pumps and  $\text{Na}^+/\text{Ca}^{2+}$  exchangers (2).

Similarly,  $\text{Ca}^{2+}_{\text{cyt}}$  regulates the physiology of plant cells. Several cellular aspects are affected, including phototropism and geotropism (3), ion fluxes in the vacuole (tonoplast) and plasma membrane (4), and photosynthesis (5). It has been postulated that increases in  $\text{Ca}^{2+}_{\text{cyt}}$  in plant cells can be induced by inositol 1,4,5-trisphosphate ( $\text{InsP}_3$ )-stimulated  $\text{Ca}^{2+}$  channels found in the tonoplast (6). Decreases in the

amount of  $\text{Ca}^{2+}_{\text{cyt}}$  may be controlled by plasma membrane-bound  $\text{Ca}^{2+}$  pumps (7) and tonoplast-bound  $\text{H}^+/\text{Ca}^{2+}$  antiports (8); the latter would sequester  $\text{Ca}^{2+}$  inside the vacuole. Here, we describe voltage-dependent channels that allow the movement of  $\text{Ba}^{2+}$  (used as a  $\text{Ca}^{2+}$  analog) into the vacuole of sugar beet cells.

Currents carried by  $\text{Ba}^{2+}$  (9) were recorded in the whole vacuole as well as in isolated outside-out patches of tonoplast (10). Vacuolar currents showed a strong inward rectification, that is, the magnitudes of the currents elicited by negative polarization of the vacuole were much larger than those elicited by positive polarization (Fig. 1A). Whole-vacuole inward currents reached steady state 2 to 3 s after the onset of the voltage pulse. When  $\text{BaCl}_2$  was substituted by KCl on the cytoplasmic side of the vacuoles and the concentration of  $\text{Ca}^{2+}_{\text{cyt}}$  was less than  $10^{-5}$  M (11), voltage pulses of between  $-100$  and  $+100$  mV elicited only small instantaneous currents (Fig. 1A, bottom). Thus, the inward rectification obtained with  $\text{BaCl}_2$  is the result of  $\text{Ba}^{2+}$  moving into the vacuole and is not due to the movement of vacuolar  $\text{Cl}^-$  in the opposite direction. With vacuoles

exposed to symmetrical  $\text{BaCl}_2$  solutions, inward currents were not observed, suggesting that intravacuolar  $\text{Ba}^{2+}$  may have blocked these currents (12). Positive potentials elicited only small outward currents under both conditions (Fig. 1B). The magnitude of the inward currents, however, increased as the tonoplast potential was made more negative. The similarity of the results from both  $\text{Ba}^{2+}$  concentrations in Fig. 1B indicates that the currents may have reached saturation. The currents elicited in vacuoles exposed to the 100 mM KCl bathing solution were of smaller magnitude than those with  $\text{Ba}^{2+}$  and varied linearly in the range of voltage studied.

Calculations from the Boltzmann plot (Fig. 1C) indicate that the  $\text{Ba}^{2+}$  currents are less sensitive to the electric field across the vacuole than the  $\text{Ca}^{2+}$  currents in animal cells where the slope  $z = 4$  (13). These results also suggest that the vacuolar  $\text{Ba}^{2+}$  currents require more energy to change from the closed to the open state, as compared to  $\text{K}^+$  currents from the sarcoplasmic reticulum of muscle cells, where the Gibbs free energy  $\Delta G_i = 1.56$  kcal  $\text{mol}^{-1}$  (14).

An estimate of the selectivity of the channels was obtained by the tail-currents method (Fig. 2). Inward currents reversed at 10 mV ( $E_{\text{rev}}$ ) with 30 mM  $\text{Ba}^{2+}$  in the cytoplasmic side and 100 mM  $\text{K}^+$  in the vacuole. Similar values were obtained from five different vacuoles. With this value of  $E_{\text{rev}}$  and using a modification of the Goldman-Hodgkin-Katz equation (15), we calculated a permeability ratio  $P_{\text{Ba}^{2+}}/P_{\text{K}^+}$  of 2.3.

Currents inactivated within 10 min, thus preventing further characterization of the inward currents (Fig. 2C). The magnitude of the currents elicited by the activating voltage pulse to  $-100$  mV decreased as the

Centre for Plant Biotechnology, Department of Botany, University of Toronto, Toronto, Ontario, Canada M5S 3B2.

\*To whom correspondence should be addressed.